ACS APPLIED MATERIALS & INTERFACES

Research Article

www.acsami.org

Constructing Uniform Core–Shell PPy@PANI Composites with Tunable Shell Thickness toward Enhancement in Microwave Absorption

Chunhua Tian,[†] Yunchen Du,[*,†,‡,∥] Ping Xu,[†] Rong Qiang,[†] Ying Wang,[†] Ding Ding,[†] Jianlei Xue,[#] Jun Ma,[‡] Hongtao Zhao,[*,∥,⊥] and Xijiang Han[*,†]

[†]Department of Chemistry, Harbin Institute of Technology, Harbin 150001, China

[‡]State Key Laboratory of Urban Water Resource and Environment, School of Municipal and Environmental Engineering, Harbin Institute of Technology, Harbin 150001, China

[∥]HIT-HAS Laboratory of High-Energy Chemistry and Interdisciplinary Science, Harbin Institute of Technology, Harbin 150001, China

[⊥]Institute of Technical Physics, Heilongjiang Academy of Sciences, Harbin 150009, China

[#]Physics Section, Medical Technology Department, Qiqihar Medical University, Qiqihar, Heilongjiang 161006, China

Supporting Information

ABSTRACT: Highly uniform core–shell composites, polypyrrole@polyaniline (PPy@PANI), have been successfully constructed by directing the polymerization of aniline on the surface of PPy microspheres. The thickness of PANI shells, from 30 to 120 nm, can be well controlled by modulating the weight ratio of aniline and PPy microspheres. PPy microspheres with abundant carbonyl groups have very strong affinity to the conjugated chains of PANI, which is responsible for the spontaneous formation of uniform core–shell microstructures. However, the strong affinity between PPy microspheres and PANI shells does not promote the diffusion or reassembly of two kinds of conjugated chains. Coating PPy microspheres with PANI shells increases the complex permittivity and creates the mechanism of interfacial polarization, where the latter plays an important role in increasing the dielectric loss of PPy@PANI composites. With a proper thickness of PANI shells, the moderate dielectric loss will produce well matched characteristic impedance, so that the microwave absorption properties of these composites can be greatly enhanced. Although PPy@PANI composites herein consume the incident electromagnetic wave by absolute dielectric loss, their performances are still superior or comparable to most PANI-based composites ever reported, indicating that they can be taken as a new kind of promising lightweight microwave absorbers. More importantly, microwave absorption of PPy@PANI composites can be simply modulated not only by the thickness of the absorbers, but also the shell thickness to satisfy the applications in different frequency bands.

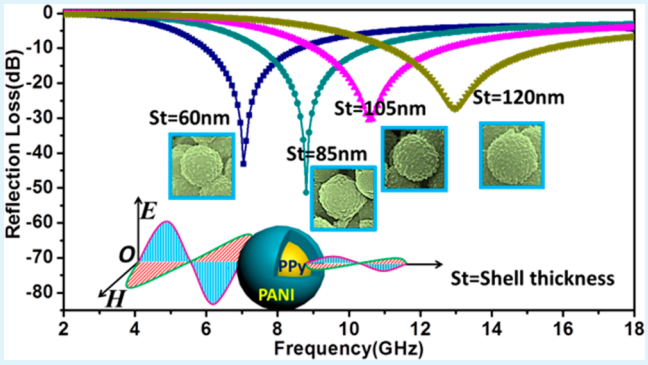

KEYWORDS: *polypyrrole@polyaniline, core–shell, shell thickness, microwave absorption, interfacial polarization*

1. INTRODUCTION

Microwave absorbing materials have received more and more attention in the past decade, not only for their significance as the key to stealth technology in military field, but also for their effective frequency regulation on excessive electromagnetic interference and electromagnetic pollution in civil field.[1,2] Traditional microwave absorbing materials such as magnetic metals and ferrites are always constrained by their high specific gravity and narrow frequency range. To satisfy the requirements of practical applications, an eligible microwave absorbing material should be labeled with some characteristic features, including lightweight, thin thickness, powerful absorption, and wide frequency bandwidth.[3] It is widely accepted that some conventional mixed composites cannot be qualified as the next generation of microwave absorbing materials, and a rational design on nanoscaled heterostructures is always necessary to produce enhanced performance. Recent progress indicates that uniform core–shell heterostructures may contribute to microwave absorption greatly due to their interfacial polarization, confinement effect, and complementary behavior.[4] In addition, the ordered microstructure and homogeneous chemical composition of uniform core–shell nanocomposites will be

Received: June 13, 2015
Accepted: August 31, 2015
Published: August 31, 2015

DOI: 10.1021/acsami.5b05259
ACS Appl. Mater. Interfaces 2015, 7, 20090–20099

also helpful to functional reproducibility and processability. As a result, various uniform core−shell nanocomposites with excellent microwave absorption, e.g., Fe_3O_4@C, Fe_3O_4@TiO_2, Fe@SiO_2, Ni@Al_2O_3, Zn@ZnO, CNCs@Al_2O_3@Fe_3O_4, and α-Fe_2O_3@$CoFe_2O_4$, are being extensively developed.[5−19]

As a typical conductive polymer, polyaniline (PANI) has been considered as a potential candidate as microwave absorbing materials due to their high conductivity, low density, ease of preparation, and good environmental stability.[20,21] In previous works, PANI was frequently employed as one of effective components in microwave absorbing composites, where PANI could not only serve as organic binder and protection coating, but also improve dielectric loss and impedance matching.[22−31] By considering the advantages of uniform core−shell heterostructures,[5−19] there is also an increasing interest in constructing uniform core−shell composites by using PANI as shells to further improve their microwave absorption properties. For example, Wang et al. deposited PANI layers on the surface of α-MoO_3 nanorods with an extremely low concentration of aniline monomers (less than 0.02 mol/L), and the enhanced microwave absorption of this novel core−shell composite was confirmed to be linked with their structural characteristics;[32] Sun et al. reported the synthesis of well dispersed core−shell Fe_3O_4@PANI nanoparticles with a very thin PANI coating (ca. 2 nm), whose absorption was significantly improved as compared with bare Fe_3O_4 nanoparticles;[33] our group also designed high-performance microwave absorbing composites, Fe_3O_4@PANI microspheres, with tunable thickness of PANI shells, where magnetic separation for the purification of uniform Fe_3O_4@PANI microspheres was necessarily applied.[34] It has been reported that inorganic particles could play the role of the nucleation sites for PANI,[35−37] while the interaction between nucleation sites and aniline monomers is weak, and thus independent PANI and core−shell composites were usually produced simultaneously. This fact will deteriorate the homogeneous chemical composition of uniform core−shell composites, resulting in poor functional reproducibility, so that aforementioned successful examples had to employ some additional strategies, e.g., dilute polymerization, surface modification, and magnetic purification, to restrain or exclude the formation of independent PANI.[32−34]

In this article, we demonstrated the refinement of uniform core−shell PANI-based composites by choosing polypyrrole (PPy) microspheres as cores for the first time. Compared with those inorganic particles, PPy microspheres have much stronger affinity to aniline monomers, as pyrrole and aniline are homologous organic molecules, which can even be homogeneously polymerized at molecular level to produce poly(aniline-*co*-pyrrole).[38] Thanks to this kind of strong affinity, uniform core−shell PPy@PANI composites can be formed automatically without any assisted methods or techniques, and the polymerization of independent PANI is also avoided effectively. The thickness of PANI shells can be easily controlled by changing the amount of aniline monomers. More importantly, the uniform core−shell PPy@PANI composites exhibit significantly enhanced microwave absorption properties, which are superior to those of pristine PANI and physically mixed PPy/PANI. The characteristic advantages of these core−shell PPy@PANI composites, e.g., easy preparation, strong absorption, wide responding range, and ultralow density (free of inorganic particles), may promise them a bright prospect as novel microwave absorbing materials.

2. EXPERIMENTAL SECTION

2.1. Synthesis of PPy Microspheres. PPy microspheres were prepared according to a previous literature.[39] Briefly, 0.1 g of $FeCl_2 \cdot 4H_2O$ was dissolved in 60 mL of distilled water, where 1.0 mL of pyrrole monomer had already been predispersed. Followed by addition of 5 mL of H_2O_2 to the pyrrole/$FeCl_2 \cdot 4H_2O$/H_2O mixture, pyrrole polymerization was initiated. The mixture was continuously stirred at room temperature for 12 h. The dark precipitated PPy was collected by centrifugation, washed with acetone several times, and finally dried at 60 °C for 12 h.

2.2. Synthesis of Core−Shell PPy@PANI Microspheres. The core−shell PPy@PANI microspheres were synthesized by an in situ polymerization method. In a typical recipe, 0.4 g of as-prepared PPy microspheres was dispersed in 100 mL of 0.1 M HCl solution under ultrasonication for 1h to obtain a uniform suspension. Required amounts of aniline monomers were then introduced into this suspension. The mixed solution was mechanically stirred in an ice−water bath for 1 h before adding ammonium persulfate (APS) for oxidative polymerization for 24 h. The precipitated powder was filtrated and washed with distilled water and ethanol until the filtrate became colorless and then dried in a vacuum drying cabinet at 70 °C. Through the experiments, the molar ratio of aniline monomers to APS was fixed at 1:1.2. To confirm that all sample, including PPy microspheres, PPy@PANI composites and pristine PANI, were sufficiently doped with HCl, the dried powders were redispersed in 0.1 M HCl for 24 h and collected by filtration and drying again. The final products were denoted as PPy@PANI-*x*, where *x* represented the mass ratio of aniline monomers to PPy microspheres. For example, PPy@PANI-0.8 and PPy@PANI-2.0 meant that 0.32 and 0.80 g of aniline monomers were involved into the reaction system, respectively.

2.3. Characterization. Scanning electron microscope (SEM) images were obtained on an HELIOS NanoLab 600i (FEI), and the samples were mounted on aluminum studs by using adhesive graphite tape and sputter coated with gold before analysis. FT-IR spectroscopy was carried out on a Nicolet Avatar 360 FT-IR spectrometric analyzer with KBr pellets. UV/vis spectra were recorded on a PUXI TU-1901 spectrophotometer by dissolving PPy@PANI microspheres in *N*-methylpyrrolidone (NMP). The conductivity of samples was measured using a KDY-1 four-point probe analyzer. Before the test, the products were dried in a vacuum oven overnight and then pressed into disks at room temperature. An Angilent PNA-N5244A microwave vector network analyzer was applied to determine the relative permeability and permittivity in the frequency range of 2−18 GHz for the calculation of reflection loss (R_L). A sample containing 50 wt % of obtained composites was pressed into a ring with an outer diameter of 7 mm, an inner diameter of 3 mm, and a thickness of 2 mm for microwave measurement in which paraffin wax was used as the binder. The reflection loss, R_L (dB), of an absorber can be deduced from the transmission line theory,

$$R_L(\mathrm{dB}) = 20\lg\left|\frac{Z_{in} - 1}{Z_{in} + 1}\right| \quad (1)$$

where Z_{in} refers to the normalized input impedance of a metal-backed microwave absorbing layer and is calculated by the following equation:[21,40]

$$Z_{in} = \sqrt{\frac{\mu_r}{\varepsilon_r}}\tanh\left[j\left(\frac{2\pi}{c}\right)fd\sqrt{\mu_r\varepsilon_r}\right] \quad (2)$$

where ε_r ($\varepsilon_r = \varepsilon_r' - j\varepsilon_r''$) and μ_r ($\mu_r = \mu_r' - j\mu_r''$) are the complex permittivity and permeability, respectively, of the composite medium, c is the velocity of electromagnetic waves in free space, f is the frequency of microwave, and d is the thickness of absorbers.

3. RESULTS AND DISCUSSION

The strategy for synthesizing core−shell PPy@PANI composites is schematically depicted in Figure 1. First, uniform PPy microspheres were prepared by a green-nano approach, where

DOI: 10.1021/acsami.5b05259
ACS Appl. Mater. Interfaces 2015, 7, 20090−20099

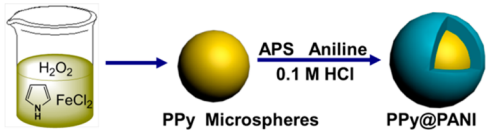

Figure 1. Schematic illustration of preparing core−shell PPy@PANI composites.

only pyrrole monomers, H_2O_2, and a small amount of $FeCl_2$ were involved.[39] Second, the core−shell PPy@PANI composites were generated by employing the as-prepared PPy microspheres as nucleation sites for the polymerization of aniline monomers. Figure 2 shows the morphology evolution of

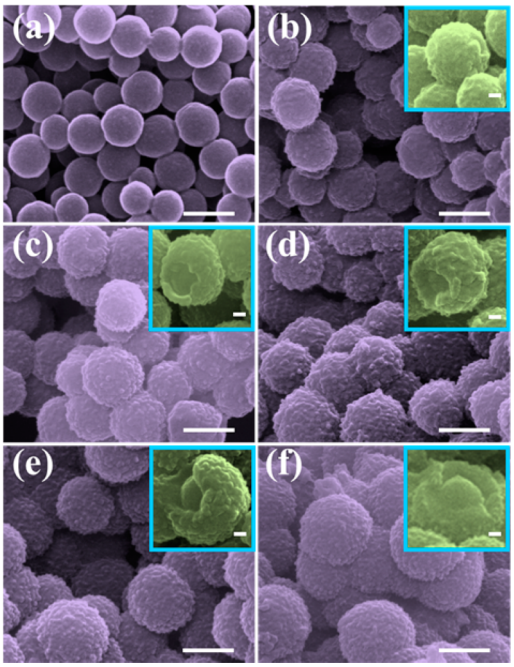

Figure 2. SEM images of PPy microspheres (a) and core−shell PPy@PANI composites with different PANI content: PPy@PANI-0.4 (b), PPy@PANI-0.8 (c), PPy@PANI-1.2 (d), PPy@PANI-1.6 (e), and PPy@PANI-2.0 (f). Inset is the high-resolution image. The scale bars in SEM images and insets are 500 and 100 nm, respectively.

PPy@PANI-*x* with different mass contents of PANI. The as-prepared PPy powder shows well-defined microspheres with very smooth surface and an average diameter of about 440 nm (Figure 2a), which is quite coincident with the previous report.[39] It is very interesting that the surface of the obtained composites becomes rough with some small bulges as compared with pristine PPy microspheres (Figure 2b−f), and their average diameters also present a monotonic increase when more aniline monomers are applied in the experiments, implying the formation of a new PANI shell. From some broken microspheres, unique core−shell structures with an interior core and an outer shell can be clearly observed (Figure 2b−f, inset). However, the interfaces between PPy microspheres and PANI shells are difficult to be identified even by high-resolution TEM due to their similar chemical composition (Figure S1). Low-magnification SEM images further suggest that the obtained composites possess highly uniform spherical microstructures (Figure S2), and impurities will not be detected until the mass ratio of PPy microspheres to aniline monomers reaches 1:2, which demonstrates that this amount of aniline monomers is excessive and random polymerization cannot be restrained with more aniline. Based on the statistical data of diameter (Figure S2), the average diameters for PPy@PANI-0.4, PPy@PANI-0.8, PPy@PANI-1.2, PPy@PANI-1.6, and PPy@PANI-2.0 are 500, 560, 610, 650, and 680 nm, respectively. That is, the average shell thicknesses for these core−shell composites are about 30, 60, 85, 105, and 120 nm. These results indicate that, with proper control of the experimental conditions and relative ratios of aniline monomers to PPy microspheres, PANI shells can be successfully fabricated on the cores and more importantly, the shell thickness is tunable at the nanoscale. In view of the fact that PPy and PANI are homologous organic polymers, it is not easy to differentiate them exactly, and therefore, gravimetric analysis is utilized to estimate the content of PANI in these composites. For all PPy@PANI composites, PPy microspheres in the solution is fixed at 0.4 g, and the final weights for PPy@PANI-0.4, PPy@PANI-0.8, PPy@PANI-1.2, PPy@PANI-1.6, and PPy@PANI-2.0 are 0.44, 0.62, 0.83, 0.98, and 1.18 g, respectively. Of note is that the total weights of PPy@PANI-0.4 and PPy@PANI-0.8 are a little far away from their theoretical outputs (0.56 and 0.72 g), which may result from the incomplete polymerization of aniline monomers and the loss of PPy microspheres. However, this situation can be inhibited in PPy@PANI-1.2, PPy@PANI-1.6 and PPy@PANI-2.0 due to the relatively high concentration of aniline monomers, so that their yields can reach about 95%, suggesting that the real compositions in these composites are approximate to those designed values.

Very interestingly, PANI obtained in the absence of PPy microspheres shows completely disordered microstructures with irregular aggregates (Figure S3), which is a hint that PPy microspheres play an important role in the direction of PANI growth. It has been accepted that the polymerization of aniline monomers could be conducted on the surface of some inorganic/organic particles with various morphology, e.g., nanofibers, nanorods, and nano/microspheres, to generate different core−shell composites. However, dilute monomers, surface modification, and assisted surfactants were always necessary to suppress random polymerization of independent PANI and promise high quality of uniform core−shell structure.[32−34] Despite that, the content of PANI is usually limited in a relatively small range, because independent PANI will appear inevitably and destroy the uniform microstructure with increasing the PANI content. For example, our group previously obtained Fe_3O_4@PANI microspheres by repeated magnetic purification, where the maximum content of PANI to produce uniform core−shell structure is less than 30 wt %.[34] However, in the current study, when PPy microspheres are applied as the cores of PANI-based composites, highly uniform core−shell composites can be produced without any additional surfactants or modification, and the content and shell thickness of PANI can reach up to about 60 wt % and 120 nm, respectively, which manifests the unique advantages of PPy microspheres as nucleation cores.

Figure 3 shows the FT-IR spectra of PPy microspheres and PPy@PANI-*x* composites with different mass contents of PANI. For PPy microspheres (Figure 3a and Figure S4), some weak characteristic peaks of PPy, such as the C−N stretching vibration in the ring (1350 cm^{-1}), the = C−H in-plane deformation modes (1270 cm^{-1}), the NH^+ in-plane deformation vibration (1097 cm^{-1}), the C−H and N−H in-plane deformation vibrations (1047 cm^{-1}), the C−C out-of-plane ring deformation vibration (960 cm^{-1}), and the C−H out-of-

DOI: 10.1021/acsami.5b05259
ACS Appl. Mater. Interfaces 2015, 7, 20090−20099

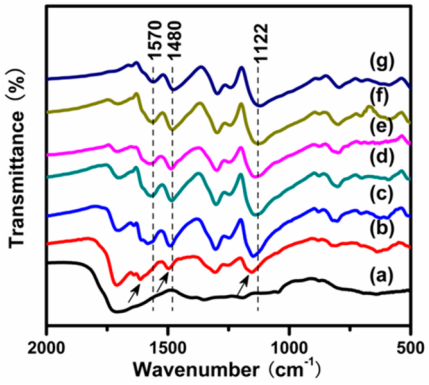

Figure 3. FT-IR spectra of PPy microspheres (a), PPy@PANI-0.4 (b), PPy@PANI-0.8 (c), PPy@PANI-1.2 (d), PPy@PANI-1.6 (e), PPy@PANI-2.0 (f), and pristine PANI (g).

plane deformation vibration of the ring (880 cm^{-1}), can be observed, indicating the formation of PPy in the first step.[41−43] Notably, there is also a very strong peak centered at 1706 cm^{-1}, and its existence covers the vibrations of aromatic C═C in pyrrole ring (about 1540 cm^{-1}) and shifts the C−C in pyrrole ring vibration from about 1450 to 1410 cm^{-1}. According to previous literature,[44,45] this peak can be assigned to carbonyl species in pyrrolidone end groups, which arises from the hydroxyl functionality introduced by the nucleophilic attack of water and the subsequent conversion of carbonyl by keto−enol tautomerism. These results suggest that PPy microspheres in our case possess relatively low polymerization degree. In contrast, the fundamental vibrations of PANI, including C═C stretching deformations of quinoid (1570 cm^{-1}) and benzenoid rings (1480 cm^{-1}), the C−N stretching of secondary aromatic amine (1295 and 1238 cm^{-1}), the aromatic C−H in-plane bending (1122 cm^{-1}), and the out-of-plane deformation of C−H in the 1,4-disubstituted benzene ring (798 cm^{-1}), are highly distinguishable in PPy@PANI-*x* composites, further confirming that the new shells formed on the surface of PPy microspheres are composed of PANI. It is unexpected that some fundamental vibrations of PANI, especially at 1570, 1480, and 1122 cm^{-1} (marked by the black arrows), in PPy@PANI-0.4 and PPy@PANI-0.8 show remarkably shifts to higher wavenumbers. These shifts, resulted from the increased energy level of internal phenyl ring, are clear signals to indicate the interaction between PPy microspheres and PANI shells.[46] For comparison, we replace PPy microspheres in PPy@PANI-0.8 with conventional PPy particles (ammonium persulfate as oxidants) and examine the FT-IR spectrum of this control composite (C-PPy@PANI-0.8, Figure S5). Although the control composite also presents some shifts at the vibrations mentioned above, the relative offsets of these shifts are still smaller than those in PPy@PANI-0.8, suggesting that PPy microspheres herein are favorable for the stronger interaction. By considering that the structure of PPy microspheres is a little different from conventional PPy particles, it is reasonable to attribute the stronger interaction in PPy@PANI-0.8 to the abundant carbonyl species of PPy microspheres, where oxygen species may lead to the formation of substantial hydrogen bonds with the conjugated chains of PANI. This is the essential fact that PPy microspheres can stimulate the formation of uniform core−shell PPy@PANI composites spontaneously. However, when more PANI is applied in the PPy@PANI-*x* composites, the shifts assigned to the interaction between PPy microspheres and PANI shells will be gradually concealed, and the composites will show identical spectra to pristine PANI.

The UV/vis absorption spectra of PPy microspheres and PPy@PANI-*x* composites with different mass contents of PANI are also investigated. As shown in Figure 4, PPy microspheres

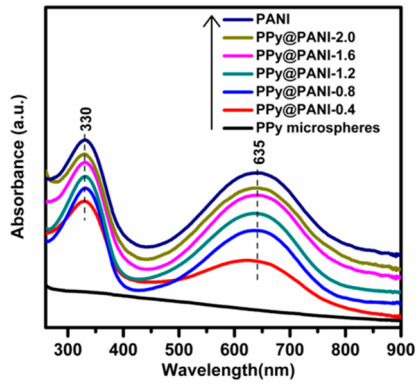

Figure 4. UV/vis spectra of PPy microspheres, PPy@PANI composites, and pristine PANI.

do not exhibit any absorption bands since their solubility in *N*-methyl pyrrolidone (NMP) is rather limited. When the PANI shells are formed on the surface of PPy microspheres, all PPy@PANI-*x* composites will display two obvious bands at about 330 and 635 nm, which can be attributed to the $\pi-\pi^*$ transition of the benzenoid ring and the benzenoid-quinoidexcitonic transition, respectively.[38] Although the interaction between PPy microspheres and PANI shells is very strong, the formation of copolymers of aniline and pyrrole in these composites has not been detected, as proved by the fact that all PPy@PANI-*x* composites inherit the basic profile of absorption bands from pristine PANI without any visible difference, even for PPy@PANI-0.4 with low PANI content.[47] In addition, it is generally accepted that the change of conjugated chains of PANI, including length and oxidation state, can produce some shifts in UV/vis absorption spectrum,[21] while the peak positions of all PPy@PANI-*x* composites in our case are almost identical to those of pristine PANI, indicating that the presence of PPy microspheres has little impact on the polymerization of aniline monomers. Based on the details of FT-IR and UV/vis spectra, the microstructure of these composites can be depicted as a simple core−shell model, and the strong interaction between cores and shells does not promote the diffusion or reassembly of two kinds of conjugated chains.

Microwave absorption properties of an absorber are highly associated with its complex permittivity and complex permeability, where the real parts of complex permittivity (ε_r') and complex permeability (μ_r') represent the storage capability of electric and magnetic energy, and imaginary parts (ε_r'' and μ_r'') stand for the loss capability of electric and magnetic energy.[6,21] Figure 5 shows the complex permittivity of PPy microspheres, PPy@PANI-*x* composites and pristine PANI in the frequency range 2−18 GHz. Although PPy is usually taken as a kind of dielectric loss material with moderate complex permittivity,[41] bare PPy microspheres in our case present almost unchanged ε_r' and ε_r'' throughout the whole frequency range, especially that their ε_r'' values are very close to zero, implying very poor dielectric loss of PPy microspheres. In general, conductivity is considered to be related with the complex permittivity to a certain degree, although it cannot

DOI: 10.1021/acsami.5b05259
ACS Appl. Mater. Interfaces 2015, 7, 20090−20099

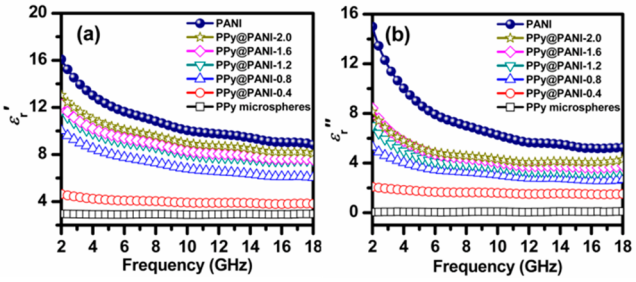

Figure 5. Real parts (a) and imaginary parts (b) of the complex permittivity of PPy microspheres, PPy@PANI composites, and pristine PANI in the frequency range of 2−18 GHz.

illustrate the dielectric behaviors directly. When the conductivity of PPy microspheres is evaluated, we are surprised to find that these PPy microspheres possess a quite low conductivity, so that it cannot be detected by four-point probe analyzer (Table S1). It is widely accepted that the conductivity of conductive polymers is mainly affected by dopants and conjugation length,[48,49] while PPy microspheres are predoped with HCl before the conductivity test, thus the poor conductivity can be reasonably attributed to their low polymerization degree, as proved by FT-IR spectra (Figure 3). Based on these results, it can be concluded that the low polymerization degree should be responsible for the difference in dielectric loss between PPy microspheres and conventional PPy powder. With the increase of PANI content, both ε_r' and ε_r'' of PPy@PANI-x composites are obviously enhanced and display typical frequency dispersion behaviors similar to those of pristine PANI. For example, the ε_r' values of PPy@PANI-0.4, PPy@PANI-0.8, PPy@PANI-1.2, PPy@PANI-1.6, and PPy@PANI-2.0 decrease from 4.64 to 3.82, 10.02 to 6.04, 11.74 to 7.45, 12.26 to 7.54, and 13.05 to 8.09, respectively; and the corresponding ε_r'' values decline from 1.08 to 0.52, 5.30 to 2.67, 7.03 to 3.46, 8.43 to 3.79, and 8.14 to 4.29, respectively. To exclude the change of PPy microspheres during the process of aniline polymerization, we designed an experiment by treating the PPy microspheres through a procedure identical to the synthesis of PPy@PANI-1.2, but no aniline monomers are added. The treated PPy microspheres present rather limited improvement in the complex permittivity (Figure S6a), far away from that endowed by the PANI shells, indicating that PANI shells are primarily responsible for the enhanced complex permittivity. In addition, FT-IR spectra also reveal that there is no obvious difference in the structure of PPy microspheres before and after APS treatment (Figure S6b), especially the treated PPy microspheres still show a very strong peak indexed as carbonyl species in pyrrolidone end groups, which again confirms the less impact of APS on PPy microspheres. The contribution of PANI shells to the complex permittivity may be explained by two aspects: conductivity and dipole orientation polarization. First, PANI has a higher conductivity than low polymerized PPy microspheres, and thus coating PANI shells on the surface of PPy microspheres can lead to the increase in the conductivity of composites (Table S1), which is favorable for enhancing the complex permittivity according to the free electron theory.[50] Fine-tuning the PANI dopant percentage may better control the conductivity and complex permittivity of the composites, while dopant percentage cannot be easily determined, thus all samples are doped with HCl for 24 h to achieve fully doped state and eliminate the influence from dopant percentage. Second, with the increase in frequency, the dipoles present in the system cannot reorient themselves along with the applied electric field. As a result, the complex permittivity starts to decrease and presents typical frequency dispersion behaviors.[51] Above results indicate that PANI plays a dominant role in determining the dielectric loss properties of these composites. In addition, it can be found that all PPy@PANI-x composites, as well as PPy microspheres and pristine PANI are unable to generate magnetic loss because of the absence of magnetic components, where the values of μ_r' and μ_r'' are approximate constants and close to 1 and 0, respectively (Figure S7).

On the basis of the measured data of the complex permittivity and complex permeability, the microwave absorption properties of PPy@PANI-x composites can be deduced according to eqs 1 and 2. Figure 6 shows their

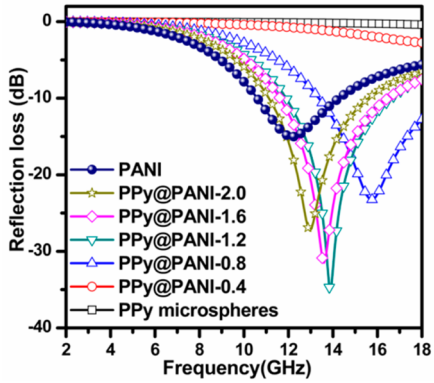

Figure 6. Reflection loss curves of PPy microspheres, PPy@PANI composites, and pristine PANI with an absorber thickness of 2 mm in the frequency range of 2−18 GHz.

reflection loss curves with a thickness of 2 mm in the frequency range of 2−18 GHz, which demonstrates that the reflection loss characteristics are sensitive to the thickness of PANI shell. PPy microspheres exhibit a reflection loss of 0 dB in the whole frequency range due to their very poor dielectric loss and magnetic loss (Figure 5 and Figure S7). Although PPy@PANI-0.4 with a relatively thin PANI shell (30 nm) has slightly improved reflection loss properties, its maximum reflection loss is still less than −5 dB. If the thickness of PANI shell is further increased, the reflection loss properties toward incident electromagnetic waves of PPy@PANI-x composites will be substantially enhanced and the frequency relating to the maximum reflection loss will be also shifted negatively. As observed, the maximum reflection losses of PPy@PANI-0.8, PPy@PANI-1.2, PPy@PANI-1.6, and PPy@PANI-2.0 are −23.3, −34.8, −31.5, and −27.3 dB at 15.8, 13.9, 13.6, and 12.9 GHz, respectively, and the bandwidths exceeding −10 dB (90% absorption) for these composites are 13.5−18.0, 11.9−16.6, 11.7−16.5, and 11.1−15.6 GHz. Both the maximum values and the responding bandwidths of these composites are absolutely superior to those of pristine PANI (−15.0 dB at 12.2 GHz, 10.6−14.2 GHz). In Table 1, we list the reflection loss properties of some typical PANI-based composites reported in recent years,[21−24,29−34,52−57] and it is clear that the enhanced microwave absorbing abilities of uniform core−shell composites, PPy@PANI-0.8, PPy@PANI-1.2, and PPy@PANI-1.6, are indeed superior or at least comparable to those composites, indicating their appreciable microwave absorption properties. It has to be mention that such good performance of core−shell

DOI: 10.1021/acsami.5b05259
ACS Appl. Mater. Interfaces 2015, 7, 20090−20099

Table 1. Microwave Absorbing Properties of Various PANI-Based Composites in Previous References and This Work (Absorber Thickness d = 2 mm)

absorbers	thickness (mm)	max RL (Frequency)	bandwidth over −10 dB (GHz)	effective bandwidth (GHz, RL <−10 dB)	ref
PANI nanoparticles	2.0	−18.8 dB (17.2 GHz)	14.1−18.0	3.9	21
$BaFe_{12}O_{19}$ /PANI	2.0	−19.7 dB (14.6 GHz)	13.0−16.9	3.9	22
$Ba(CoTi)_xFe_{12-2x}O_{19}$/PANI	2.0	−33.7 dB (14.6 GHz)	12.0−17.3	5.3	23
Fe_3O_4 microspheres/PANI	2.0	−18.6 dB (14.0 GHz)	12.1−16.0	3.9	24
Fe_3O_4/MWCNT/PANI	2.0	−8.0 dB (14.7 GHz)	Undetected	0	29
graphite/$CoFe_2O_4$/PANI	2.0	−11.0 dB (3.8 GHz)	3.4−4.0	0.6	30
graphene/PANI	2.0	−25.3 dB (16.5 GHz)	13.9−18.0	4.1	31
α-MoO_3 /PANI	2.0	−33.7 dB (16.9 GHz)	14.2−18.0	3.8	32
Fe_3O_4/PANI	2.0	−13.8 dB (16.7 GHz)	16.3−17.2	0.9	33
Fe_3O_4 microspheres/PANI	2.0	−37.4 dB (15.4 GHz)	13.0−18.0	5.0	34
NiZn ferrite/PANI	2.0	−20.0 dB (14.0 GHz)	12.0−16.6	4.6	52
Fe_3O_4/CIP/PANI	2.0	−25.5 dB (10.1 GHz)	7.1−9.9	2.8	53
$BaTiO_3$/PANI	2.0	−13.8 dB (11.6 GHz)	10.7−12.5	1.8	54
MnO_2/PANI	2.0	−20.9 dB (13.5 GHz)	11.4−16.8	4.4	55
graphene@Fe_3O_4@SiO_2@PANI	2.0	−19.4 dB (16.4 GHz)	10.4−18.0	4.4	56
Ni/C/PANI	2.0	−7.5 dB (10.0 GHz)	Undetected	0	57
PPy@PANI-0.8	2.0	−23.3 dB (15.8 GHz)	13.5−18.0	4.5	Herein
PPy@PANI-1.2	2.0	−34.8 dB (13.9 GHz)	11.9−16.6	4.7	Herein
PPy@PANI-1.6	2.0	−31.5 dB (13.6 GHz)	11.7−16.4	4.7	Herein

PPy@PANI composites has been achieved without any assistance of some common metals or metal oxides, which further demonstrates their promising prospect as a new kind of lightweight microwave absorbers.

As discussed above, core−shell PPy@PANI composites have negligible magnetic loss mechanism, and therefore they attenuate the incident electromagnetic wave with single dielectric loss mechanism. Dielectric dissipation factor (tan $\delta_e = \varepsilon''/\varepsilon'$) is a common concept to evaluate the dielectric loss abilities of microwave absorbers. As shown in Figure 7, bare

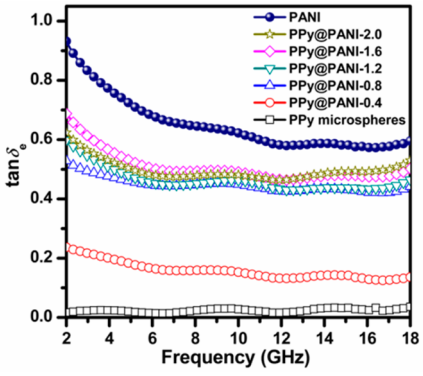

Figure 7. Dielectric dissipation factors (tan δ_e) of PPy microspheres, PPy@PANI composites, and pristine PANI in the frequency range of 2−18 GHz.

PPy microspheres show quite low tan δ_e in the whole frequency range due to its small ε'' values (Figure 5). With the formation of PANI shells on the surface of PPy microspheres, tan δ_e can be substantially enhanced from PPy microspheres to PPy@PANI-0.8. However, when the shell thickness exceeds 60 nm, increase in tan δ_e becomes slow. It is widely accepted that dielectric loss ability mainly comes from conductivity loss and polarization loss,[58,59] where the latter can be further divided as ionic polarization, electronic polarization, dipole orientation polarization and interfacial polarization (space charge polarization).[60] Ionic polarization and electronic polarization can be easily excluded because they usually occur at much higher frequency region ($10^3 \sim 10^6$ GHz).[60] Due to the higher conductivity of PANI, the conductivity loss and dipole orientation polarization will be highly dependent on the content of PANI. However, remarkable difference in the PANI content between PPy@PANI-0.8 and PPy@PANI-2.0 does not produce a big gap for their tan δ_e, implying that interfacial polarization will become the dominant mechanism for dielectric loss once the thickness of PANI shells reach a critical value. To address the advantages of core−shell structure, the investigation on a physically mixed composite (PPy/PANI-1.2) with the similar chemical composition to PPy@PANI-1.2 is also conducted (Figure S8). It is clear that PPy/PANI-1.2 exhibits much smaller complex permittivity as compared to PPy@PANI-1.2, whose ε_r'' values are less than 2.0 in the whole frequency range, which results in its inferior dielectric loss ability (Figure S9). Obviously, the change of microstructure should be responsible for this phenomenon. On one hand, the blocking of conductive PANI network by bare PPy microspheres with low polymerization degree (Figure S10) will lead to the decreased conductivity loss. It is more important that, on the other hand, the insufficient contact between PPy microspheres and PANI cannot afford enough interfacial polarization to promote the dielectric loss ability to the same level of PPy@PANI-1.2, which is consistent with previous works.[7,61,62] Based on these data, one can see that the reflection loss property of PPy/PANI-1.2 is far behind PPy@PANI-1.2 (Figure S11).

It has to point out that pristine PANI herein exhibits superior tan δ_e to these core−shell PPy@PANI composites, while it still fails to produce considerable reflection losses. This is because the reflection loss is highly related to another important parameter, the concept of matched characteristic impedance, which can determine the transmission behaviors of electromagnetic wave.[63,64] If the characteristic impedance is well matched, most of electromagnetic wave can enter into microwave absorbers to be converted into thermal energy or

DOI: 10.1021/acsami.5b05259
ACS Appl. Mater. Interfaces 2015, 7, 20090−20099

dissipated through interference; otherwise, most of electromagnetic wave will be reflected at the front surface of microwave absorbers or pass through the microwave absorbers without any dissipation. However, the normalized characteristic impedance (Z_{in}, Z_{in} equals to real input impedance divided by impedance in free space), calculated from the complex permittivity and complex permeability, is typically an imaginary number, thus it is difficult to evaluate them directly. According to eqs 1 and 2, when the modulus of Z_{in}-1 gets closer to zero, stronger reflection loss properties will be produced. To better understand the results of reflection loss properties, Figure 8

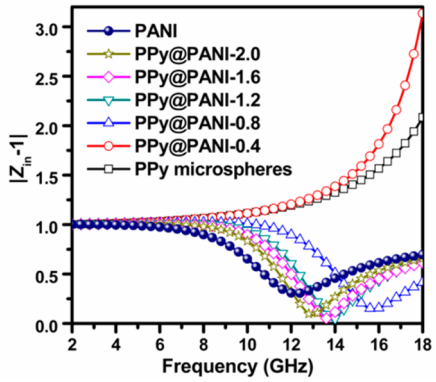

Figure 8. Modulus of Z_{in}-1 of various composites with an absorber thickness of 2 mm in the frequency range of 2−18 GHz.

shows the modulus of Z_{in}-1 of various composites with an absorber thickness of 2 mm in the studied frequency range. As observed, the modulus of Z_{in}-1 in PPy microspheres and PPy@PANI-0.4 is far away from zero, thus they cannot attenuate the incident electromagnetic wave effectively. Although the modulus of Z_{in}-1 of pristine PANI presents an approaching trend to the horizontal ordinate in the frequency range of 6−18 GHz, its minimum value is only 0.30, which is still much larger than those of PPy@PANI-0.8 (0.15), PPy@PANI-1.2 (0.04), PPy@PANI-1.6 (0.05), and PPy@PANI-2.0 (0.08). That is why pristine PANI has better complex permittivity and dielectric dissipation factor, but its reflection loss property is inferior to those of PPy@PANI composites. These results further suggest that the enhanced reflection loss properties of PPy@PANI composites can be attributed to the synergetic effect between PPy microspheres and PANI shells, where PANI shells increase the dielectric loss ability of PPy microspheres, and PPy microspheres optimize the matched characteristic impedance of PANI shells.

According to the eq 2, the thickness (d) of an absorber is also one of the crucial parameters that affects the intensity and responding frequency of reflection loss, and thus the reflection losses produced from different thicknesses (2.0, 2.5, 3.0, 4.0, and 5.0 mm) are further investigated in order to eliminate the influence of absorber thickness. As shown in Figure 9, maximum reflection losses of all core−shell PPy@PANI composites exhibit negative shifts to lower frequency with increased thickness, and very wide responding bandwidths over −10 dB (90% absorption) can be easily obtained in these composites with variation in thickness from 2.0 to 5.0 mm (Table S1), which are much better than that of pristine PANI (Figure S12), further confirming the enhancement of microwave absorption properties in these core−shell composites. A careful look at the microwave absorption curves reveals that

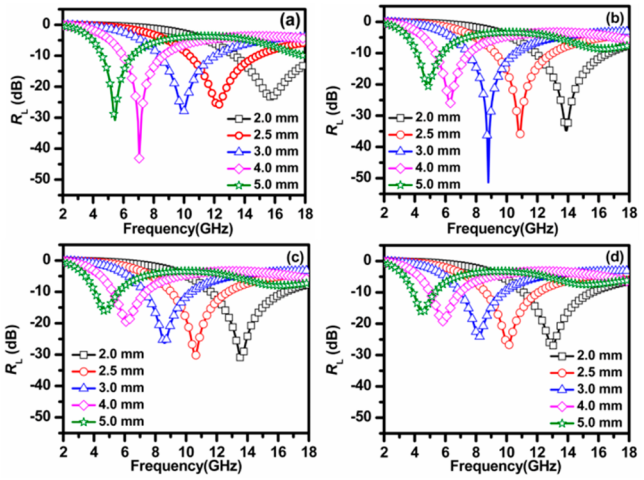

Figure 9. Microwave reflection losses of PPy@PANI-0.8 (a), PPy@PANI-1.2 (b), PPy@PANI-1.6 (c), and PPy@PANI-2.0 (d) at different absorber thicknesses.

these composites can display the strongest reflection loss in different frequency ranges, especially for PPy@PANI-0.8 and PPy@PANI-1.2, whose maximum values can reach −43.1 dB at 7.1 GHz and −51.3 dB at 8.8 GHz with a thickness of 4.0 and 3.0 mm, respectively. Such good performance is not common in previous conductive polymer-based composites (Table S2). These results substantially indicate that constructing core−shell PPy@PANI structure will be a promising route to enhance the microwave absorption properties of PANI-based composites, and more importantly, the absorption of the obtained composites can be simply modulated not only by the absorber thickness, but also by the shell thickness to satisfy the applications in different frequency bands.

4. CONCLUSIONS

With PPy microspheres as the cores and nucleation sites, core−shell PPy@PANI composites have been successfully constructed through an in situ polymerization of aniline monomers. Due to the low polymerization degree, carbonyl species in the end groups are rather rich on the surface of PPy microsphere, so that they can display strong affinity to the conjugated chains of PANI by hydrogen bonds, resulting in spontaneous formation of highly uniform core−shell microstructure without any pretreatment techniques. The thickness of PANI shells can be well controlled from 30 to 120 nm by changing the weight ratio of aniline and PPy microspheres. PPy@PANI composites show substantially enhanced microwave absorption properties as compared to PPy microspheres, pristine PANI, as well as the physically mixed PPy/PANI composites. Their excellent performances can be even better than many PANI-based composites ever reported. Investigations on the mechanism of microwave absorption indicate that interfacial polarization contributes to the dielectric loss significantly, which is beneficial to creating well matched characteristic impedance in these core−shell composites and producing strong reflection loss. More importantly, the microwave absorption properties are highly dependent on the thickness of PANI shells, which means that the microwave absorption can be simply modulated not only by manipulating the absorber thickness, but also by tuning the shell thickness to satisfy the applications in different frequency bands. We believe this work will be helpful for the design and development of

DOI: 10.1021/acsami.5b05259
ACS Appl. Mater. Interfaces 2015, 7, 20090−20099

some novel lightweight microwave absorbers with uniform microstructure and enhanced functional property.

■ ASSOCIATED CONTENT

Supporting Information

The Supporting Information is available free of charge on the ACS Publications website at DOI: 10.1021/acsami.5b05259.

TEM image of PPy@PANI-1.2; low-magnification SEM images and statistical data on diameters of PPy@PANI composites; SEM image of pristine PANI and physically mixed PPy/PANI-1.2 composite; FT-IR spectra of PPy microspheres and composites of PANI and conventional PPy nanoparticles; complex permeability of PPy@PANI composites; complex permittivity, complex permeability, and dielectric dissipation factors of core−shell PPy@PANI-1.2 and physically mixed PPy/PANI-1.2 composites; reflection loss curves of core−shell PPy@PANI-1.2, physically mixed PPy/PANI-1.2 composite, and pristine PANI at different absorber thicknesses; room-temperature electrical conductivities of PPy@PANI composites; microwave absorbing properties of various PANI-based composites in previous references and this work (PDF)

■ AUTHOR INFORMATION

Corresponding Authors

*E-mail: yunchendu@hit.edu.cn.
*E-mail: hanxijiang@hit.edu.cn.
*E-mail: zhaohongtao1976@163.com.

Notes

The authors declare no competing financial interest.

■ ACKNOWLEDGMENTS

This work is supported by National Natural Science Foundation of China (21371039, 21446006, 51377048, and 21471039), China Postdoctoral Science Foundation (2013M541394 and 2014T70341), the Program for Innovation Research of Science in HIT (B201411), Natural Science Foundation of Heilongjiang Province (B201405 and B2015001), Open Project of State Key Laboratory of Urban Water Resource and Environment, HIT (QA201414), and Harbin Technological Innovation Talent Research Special Fund (2013RFQYG170).

■ REFERENCES

(1) He, Q.; Yuan, T.; Zhang, X.; Yan, X.; Guo, J.; Ding, D.; Khan, M. A.; Young, D. P.; Khasanov, A.; Luo, Z.; Liu, J.; Shen, T. D.; Liu, X.; Wei, S.; Guo, Z. Electromagnetic Field Absorbing Polypropylene Nanocomposites with Tuned Permittivity and Permeability by Nanoiron and Carbon Nanotubes. *J. Phys. Chem. C* **2014**, *118*, 24784−24796.

(2) Sun, H.; Che, R.; You, X.; Jiang, Y.; Yang, Z.; Deng, J.; Qiu, L.; Peng, H. Cross-Stacking Aligned Carbon-Nanotube Films To Tune Microwave Absorption Frequencies And Increase Absorption Intensities. *Adv. Mater.* **2014**, *26*, 8120−8125.

(3) Zhao, T.; Hou, C.; Zhang, H.; Zhu, R.; She, S.; Wang, J.; Li, T.; Liu, Z.; Wei, B. Electromagnetic Wave Absorbing Properties Of Amorphous Carbon Nanotubes. *Sci. Rep.* **2014**, *4*, 5619.

(4) Liu, X.; Li, B.; Geng, D.; Cui, W.; Yang, F.; Xie, Z.; Kang, D.; Zhang, Z. (Fe, Ni)/C Nanocapsules For Electromagnetic-Wave-Absorber in the Whole Ku-Band. *Carbon* **2009**, *47*, 470−474.

(5) Chen, Y. J.; Xiao, G.; Wang, T. S.; Ouyang, Q. Y.; Qi, L. H.; Ma, Y.; Gao, P.; Zhu, C. L.; Cao, M. S.; Jin, H. B. Porous Fe_3O_4/Carbon Core/Shell Nanorods: Synthesis And Electromagnetic Properties. *J. Phys. Chem. C* **2011**, *115*, 13603−13608.

(6) Du, Y.; Liu, W.; Qiang, R.; Wang, Y.; Han, X.; Ma, J.; Xu, P. Shell Thickness-Dependent Microwave Absorption of Core-Shell Fe_3O_4@C Composites. *ACS Appl. Mater. Interfaces* **2014**, *6*, 12997−13006.

(7) Yuan, K. P.; Che, R. C.; Cao, Q.; Sun, Z. K.; Yue, Q.; Deng, Y. H. Designed Fabrication and Characterization of Three-Dimensionally Ordered Arrays of Core-Shell Magnetic Mesoporous Carbon Microspheres. *ACS Appl. Mater. Interfaces* **2015**, *7*, 5312−5319.

(8) Liu, J.; Che, R.; Chen, H.; Zhang, F.; Xia, F.; Wu, Q.; Wang, M. Microwave Absorption Enhancement of Multifunctional Composite Microspheres with Spinel Fe_3O_4 Cores and Anatase TiO_2 Shells. *Small* **2012**, *8*, 1214−1221.

(9) Zhu, C. L.; Zhang, M. L.; Qiao, Y. J.; Xiao, G.; Zhang, F.; Chen, Y. J. Fe_3O_4/TiO_2 Core/Shell Nanotubes: Synthesis and Magnetic and Electromagnetic Wave Absorption Characteristics. *J. Phys. Chem. C* **2010**, *114*, 16229−16235.

(10) Zhu, J.; Wei, S.; Haldolaarachchige, N.; Young, D. P.; Guo, Z. Electromagnetic Field Shielding Polyurethane Nanocomposites Reinforced with Core-Shell Fe-Silica Nanoparticles. *J. Phys. Chem. C* **2011**, *115*, 15304−15310.

(11) Zhang, X.; Huang, H.; Dong, X. Core/Shell Metal/Heterogeneous Oxide Nanocapsules: The Empirical Formation Law and Tunable Electromagnetic Losses. *J. Phys. Chem. C* **2013**, *117*, 8563−8569.

(12) Zhao, B.; Shao, G.; Fan, B.; Zhao, W.; Zhang, R. Fabrication and Enhanced Microwave Absorption Properties of Al_2O_3 Nanoflake-Coated Ni Core-Shell Composite Microspheres. *RSC Adv.* **2014**, *4*, 57424−57429.

(13) Wang, G.; Gao, Z.; Tang, S.; Chen, C.; Duan, F.; Zhao, S.; Lin, S.; Feng, Y.; Zhou, L.; Qin, Y. Microwave Absorption Properties of Carbon Nanocoils Coated with Highly Controlled Magnetic Materials by Atomic Layer Deposition. *ACS Nano* **2012**, *6*, 11009−11017.

(14) Lv, H. L.; Liang, X. H.; Cheng, Y.; Zhang, H. Q.; Tang, D. M.; Zhang, B. S.; Ji, G. B.; Du, Y. W. Coin-like alpha-Fe_2O_3@$CoFe_2O_4$ Core-Shell Composites with Excellent Electromagnetic Absorption Performance. *ACS Appl. Mater. Interfaces* **2015**, *7*, 4744−4750.

(15) Chen, Y. J.; Gao, P.; Wang, R. X.; Zhu, C. L.; Wang, L. J.; Cao, M. S.; Jin, H. B. Porous Fe_3O_4/SnO_2 Core/Shell Nanorods: Synthesis and Electromagnetic Properties. *J. Phys. Chem. C* **2009**, *113*, 10061−10064.

(16) Xu, J.; Liu, J.; Che, R.; Liang, C.; Cao, M.; Li, Y.; Liu, Z. Polarization Enhancement of Microwave Absorption by Increasing Aspect Ratio of Ellipsoidal Nanorattles With Fe_3O_4 Cores and Hierarchical $CuSiO_3$ Shells. *Nanoscale* **2014**, *6*, 5782−5790.

(17) Sun, D.; Zou, Q.; Wang, Y.; Wang, Y.; Jiang, W.; Li, F. Controllable Synthesis of Porous Fe_3O_4@ZnO Sphere Decorated Graphene for Extraordinary Electromagnetic Wave Absorption. *Nanoscale* **2014**, *6*, 6557−6562.

(18) Zhao, B.; Shao, G.; Fan, B.; Zhao, W.; Zhang, R. Investigation of the Electromagnetic Absorption Properties of Ni@TiO_2 and Ni@SiO_2 Composite Microspheres with Core-Shell Structure. *Phys. Chem. Chem. Phys.* **2015**, *17*, 2531−2539.

(19) Zhong, B.; Tang, X. H.; Huang, X. X.; Xia, L.; Zhang, X. D.; Wen, G. W.; Chen, Z. Metal-Semiconductor Zn/ZnO Core-Shell Nanocables: Facile and Large-scale Fabrication, Growth Mechanism, Oxidation Behavior, and Microwave Absorption Performance. *CrystEngComm* **2015**, *17*, 2806−2814.

(20) Wang, Y. Microwave Absorbing Materials Based on Polyaniline Composites: A Review. *Int. J. Mater. Res.* **2014**, *105*, 3−12.

(21) Zhang, P.; Han, X.; Kang, L.; Qiang, R.; Liu, W.; Du, Y. Synthesis and Characterization of Polyaniline Nanoparticles with Enhanced Microwave Absorption. *RSC Adv.* **2013**, *3*, 12694−12701.

(22) Xu, P.; Han, X.; Jiang, J.; Wang, X.; Li, X.; Wen, A. Synthesis and Characterization of Novel Coralloid Polyaniline/$BaFe_{12}O_{19}$ Nanocomposites. *J. Phys. Chem. C* **2007**, *111*, 12603−12608.

(23) Du, L.; Du, Y.; Li, Y.; Wang, J.; Wang, C.; Wang, X.; Xu, P.; Han, X. Surfactant-Assisted Solvothermal Synthesis of Ba-$(CoTi)_xFe_{12-2x}O_{19}$ Nanoparticles and Enhancement in Microwave

DOI: 10.1021/acsami.5b05259
ACS Appl. Mater. Interfaces 2015, 7, 20090−20099

Absorption Properties of Polyaniline. *J. Phys. Chem. C* **2010**, *114*, 19600−19606.
(24) Cui, C.; Du, Y.; Li, T.; Zheng, X.; Wang, X.; Han, X.; Xu, P. Synthesis of Electromagnetic Functionalized Fe_3O_4 Microspheres/Polyaniline Composites by Two-Step Oxidative Polymerization. *J. Phys. Chem. B* **2012**, *116*, 9523−9531.
(25) Saini, P.; Arora, M.; Gupta, G.; Gupta, B. K.; Singh, V. N.; Choudhary, V. High Permittivity Polyaniline-Barium Titanate Nanocomposites with Excellent Electromagnetic Interference Shielding Response. *Nanoscale* **2013**, *5*, 4330−4336.
(26) Singh, A. P.; Mishra, M.; Sambyal, P.; Gupta, B. K.; Singh, B. P.; Chandra, A.; Dhawan, S. K. Encapsulation of γ-Fe_2O_3 Decorated Reduced Graphene Oxide in Polyaniline Core-Shell Tubes as An Exceptional Tracker for Electromagnetic Environmental Pollution. *J. Mater. Chem. A* **2014**, *2*, 3581−3593.
(27) Gu, H.; Huang, Y.; Zhang, X.; Wang, Q.; Zhu, J.; Shao, L.; Haldolaarachchige, N.; Young, D. P.; Wei, S.; Guo, Z. Magnetoresistive Polyaniline-Magnetite Nanocomposites with Negative Dielectrical Properties. *Polymer* **2012**, *53*, 801−809.
(28) Gupta, T. K.; Singh, B. P.; Mathur, R. B.; Dhakate, S. R. Multi-Walled Carbon Nanotube−Graphene−Polyaniline Multiphase Nanocomposite with Superior Electromagnetic Shielding Effectiveness. *Nanoscale* **2014**, *6*, 842−851.
(29) Cao, M. S.; Yang, J.; Song, W. L.; Zhang, D. Q.; Wen, B.; Jin, H. B.; Hou, Z. L.; Yuan, J. Ferroferric Oxide/Multiwalled Carbon Nanotube vs Polyaniline/Ferroferric Oxide/Multiwalled Carbon Nanotube Multiheterostructures for Highly Effective Microwave Absorption. *ACS Appl. Mater. Interfaces* **2012**, *4*, 6949−6956.
(30) Chen, K.; Xiang, C.; Li, L.; Qian, H.; Xiao, Q.; Xu, F. A Novel Ternary Composite: Fabrication, Performance and Application of Expanded Graphite/Polyaniline/$CoFe_2O_4$ Ferrite. *J. Mater. Chem.* **2012**, *22*, 6449−6455.
(31) Yu, H.; Wang, T.; Wen, B.; Lu, M.; Xu, Z.; Zhu, C.; Chen, Y.; Xue, X.; Sun, C.; Cao, M. Graphene/Polyaniline Nanorod Arrays: Synthesis and Excellent Electromagnetic Absorption Properties. *J. Mater. Chem.* **2012**, *22*, 21679−21685.
(32) Wang, Q.; Lei, Z.; Chen, Y.; Ouyang, Q.; Gao, P.; Qi, L.; Zhu, C.; Zhang, J. Branched Polyaniline/Molybdenum Oxide Organic/Inorganic Heteronanostructures: Synthesis and Electromagnetic Absorption Properties. *J. Mater. Chem. A* **2013**, *1*, 11795−11801.
(33) Sun, Y.; Xiao, F.; Liu, X.; Feng, C.; Jin, C. Preparation and Electromagnetic Wave Absorption Properties of Core-Shell Structured Fe_3O_4-Polyaniline Nanoparticles. *RSC Adv.* **2013**, *3*, 22554−22559.
(34) Zhang, B.; Du, Y.; Zhang, P.; Zhao, H.; Kang, L.; Han, X.; Xu, P. Microwave Absorption Enhancement of Fe_3O_4/Polyaniline Core/Shell Hybrid Microspheres With Controlled Shell Thickness. *J. Appl. Polym. Sci.* **2013**, *130*, 1909−1916.
(35) Zhang, X.; Goux, W. J.; Manohar, S. K. Synthesis of Polyaniline Nanofibers by "Nanofiber Seeding. *J. Am. Chem. Soc.* **2004**, *126*, 4502−4503.
(36) Xing, S. X.; Tan, L. H.; Yang, M. X.; Pan, M.; Lv, Y. B.; Tang, Q. H.; Yang, Y. H.; Chen, H. Y. Highly Controlled Core/Shell Structures: Tunable Conductive Polymer Shells on Gold Nanoparticles and Nanochains. *J. Mater. Chem.* **2009**, *19*, 3286−3291.
(37) Xing, S. X.; Tan, L. H.; Chen, T.; Yang, Y. H.; Chen, H. Y. Facile Fabrication of Triple-Layer (Au@Ag)@Polypyrrole Core-Shell and (Au@H_2O)@Polypyrrole Yolk-Shell Nanostructures. *Chem. Commun.* **2009**, *45*, 1653−1654.
(38) Xu, P.; Han, X.; Wang, C.; Zhang, B.; Wang, X.; Wang, H. L. Facile Synthesis of Polyaniline-Polypyrrole Nanofibers for Application in Chemical Deposition of Metal Nanoparticles. *Macromol. Rapid Commun.* **2008**, *29*, 1392−1397.
(39) Liu, Z.; Liu, Y.; Poyraz, S.; Zhang, X. Green-Nano Approach to Nanostructured Polypyrrole. *Chem. Commun.* **2011**, *47*, 4421−4423.
(40) Du, Y.; Liu, T.; Yu, B.; Gao, H.; Xu, P.; Wang, J.; Wang, X.; Han, X. The Electromagnetic Properties and Microwave Absorption of Mesoporous Carbon. *Mater. Chem. Phys.* **2012**, *135*, 884−891.
(41) Xu, P.; Han, X.; Wang, C.; Zhao, H.; Wang, J.; Wang, X.; Zhang, B. Synthesis of Electromagnetic Functionalized Barium Ferrite Nanoparticles Embedded in Polypyrrole. *J. Phys. Chem. B* **2008**, *112*, 2775−2781.
(42) Blinova, N. V.; Stejskal, J.; Trchová, M.; Prokeš, J.; Omastová, M. Polyaniline and Polypyrrole: A Comparative Study of the Preparation. *Eur. Polym. J.* **2007**, *43*, 2331−2341.
(43) Bian, X.; Lu, X.; Jin, E.; Kong, L.; Zhang, W.; Wang, C. Fabrication of Pt/Polypyrrole Hybrid Hollow Microspheres and Their Application in Electrochemical Biosensing towards Hydrogen Peroxide. *Talanta* **2010**, *81*, 813−818.
(44) Antony, M. J.; Jayakannan, M. Self-Assembled Anionic Micellar Template for Polypyrrole, Polyaniline, and Their Random Copolymer Nanomaterials. *J. Polym. Sci., Part B: Polym. Phys.* **2009**, *47*, 830−846.
(45) Ravichandran, S.; Nagarajan, S.; Kokil, A.; Ponrathnam, T.; Bouldin, R. M.; Bruno, F. F.; Samuelson, L.; Kumar, J.; Nagarajan, R. Micellar Nanoreactors for Hematin Catalyzed Synthesis of Electrically Conducting Polypyrrole. *Langmuir* **2012**, *28*, 13380−13386.
(46) Deng, J.; Ding, X.; Zhang, W.; Peng, Y.; Wang, J.; Long, X.; Li, P.; Chan, A. S. Magnetic and Conducting Fe_3O_4-Cross-Linked Polyaniline Nanoparticles with Core-Shell Structure. *Polymer* **2002**, *43*, 2179−2184.
(47) Xu, P.; Han, X.; Wang, C.; Zhang, B.; Wang, H. L. Morphology and Physico-Electrochemical Properties of Poly (Aniline-co-Pyrrole). *Synth. Met.* **2009**, *159*, 430−434.
(48) Song, M. K.; Kim, Y. T.; Kim, B. S.; Kim, J.; Char, K.; Rhee, H. W. Synthesis and Characterization of Soluble Polypyrrole Doped with Alkylbenzenesulfonic Acids. *Synth. Met.* **2004**, *141*, 315−319.
(49) Yoo, J. E.; Cross, J. L.; Bucholz, T. L.; Lee, K. S.; Espe, M. P.; Loo, Y. L. Improving the Electrical Conductivity of Polymer Acid-Doped Polyaniline by Controlling the Template Molecular Weight. *J. Mater. Chem.* **2007**, *17*, 1268−1275.
(50) Zhang, X.; Dong, X.; Huang, H.; Liu, Y.; Wang, W.; Zhu, X.; Lv, B.; Lei, J.; Lee, C. Microwave Absorption Properties of the Carbon-Coated Nickel Nanocapsules. *Appl. Phys. Lett.* **2006**, *89*, 053115.
(51) Ohlan, A.; Singh, K.; Chandra, A.; Dhawan, S. K. Microwave Absorption Behavior of Core-Shell Structured Poly(3, 4-Ethylenedioxy Thiophene)-Barium Ferrite Nanocomposites. *ACS Appl. Mater. Interfaces* **2010**, *2*, 927−933.
(52) Ting, T. H.; Yu, R. P.; Jau, Y. N. Synthesis and Microwave Absorption Characteristics of Polyaniline/NiZn Ferrite Composites in 2−40 GHz. *Mater. Chem. Phys.* **2011**, *126*, 364−368.
(53) He, Z.; Fang, Y.; Wang, X.; Pang, H. Microwave Absorption Properties of PANI/CIP/Fe_3O_4 Composites. *Synth. Met.* **2011**, *161*, 420−425.
(54) Yang, C.; Gung, Y.; Hung, W.; Ting, T.; Wu, K. Infrared and Microwave Absorbing Properties of $BaTiO_3$/Polyaniline and $BaFe_{12}O_{19}$/Polyaniline Composites. *Compos. Sci. Technol.* **2010**, *70*, 466−471.
(55) Hu, J.; Duan, Y.; Zhang, J.; Jing, H.; Liu, S.; Li, W. γ-MnO_2/Polyaniline Composites: Preparation, Characterization, and Applications in Microwave Absorption. *Phys. B* **2011**, *406*, 1950−1955.
(56) Wang, L.; Zhu, J.; Yang, H.; Wang, F.; Qin, Y.; Zhao, T.; Zhang, P. Fabrication of Hierarchical Graphene@Fe_3O_4@SiO_2@Polyaniline Quaternary Composite and Its Improved Electrochemical Performance. *J. Alloys Compd.* **2015**, *634*, 232−238.
(57) Liu, X.; Or, S. W.; Leung, C. M.; Ho, S. Core/Shell/Shell-Structured Nickel/Carbon/Polyaniline Nanocapsules with Large Absorbing Bandwidth and Absorber Thickness Range. *J. Appl. Phys.* **2014**, *115*, 17A507.
(58) Lu, M. M.; Cao, W. Q.; Shi, H. L.; Fang, X. Y.; Yang, J.; Hou, Z. L.; Jin, H. B.; Wang, W. Z.; Yuan, J.; Cao, M. S. Multi-Wall Carbon Nanotubes Decorated with ZnO Nanocrystals: Mild Solution-Process Synthesis and Highly Efficient Microwave Absorption Properties at Elevated Temperature. *J. Mater. Chem. A* **2014**, *2*, 10540−10547.
(59) Wen, B.; Cao, M. S.; Hou, Z. L.; Song, W. L.; Zhang, L.; Lu, M. M.; Jin, H. B.; Fang, X. Y.; Wang, W. Z.; Yuan, J. Temperature Dependent Microwave Attenuation Behavior for Carbon-Nanotube/Silica Composites. *Carbon* **2013**, *65*, 124−139.
(60) Kittel, C. *Introduction to Solid State Physics*, 8th ed.; John Wiley & Sons, Inc.: New York, 2005.

DOI: 10.1021/acsami.5b05259
ACS Appl. Mater. Interfaces 2015, 7, 20090−20099

(61) Zhao, X. C.; Zhang, Z. M.; Wang, L. Y.; Xi, K.; Cao, Q. Q.; Wang, D. H.; Yang, Y.; Du, Y. W. Excellent Microwave Absorption Property of Graphene-Coated Fe Nanocomposites. *Sci. Rep.* **2013**, *3*, 3421.
(62) Kong, L.; Yin, X. W.; Zhang, Y. J.; Yuan, X. Y.; Li, Q.; Ye, F.; Cheng, L. F.; Zhang, L. T. Electromagnetic Wave Absorption Properties of Reduced Graphene Oxide Modified by Maghemite Colloidal Nanoparticle Clusters. *J. Phys. Chem. C* **2013**, *117*, 19701−19711.
(63) Song, W. L.; Cao, M. S.; Fan, L. Z.; Lu, M. M.; Li, Y.; Wang, C. Y.; Ju, H. F. Highly Ordered Porous Carbon/Wax Composites for Effective Electromagnetic Attenuation and Shielding. *Carbon* **2014**, *77*, 130−142.
(64) Qiang, R.; Du, Y. C.; Zhao, H. T.; Wang, Y.; Tian, C. H.; Li, Z. G.; Han, X. J.; Xu, P. Metal Organic Framework-Derived Fe/C Nanocubes toward Efficient Microwave Absorption. *J. Mater. Chem. A* **2015**, *3*, 13426−13434.

DOI: 10.1021/acsami.5b05259
ACS Appl. Mater. Interfaces 2015, 7, 20090−20099